

Kinetic studies on the decomposition of potassium bis(oxalato)cobaltate(II)

J.E. House, Jr. * and P.-L. Ho

Department of Chemistry, Illinois State University, Normal, IL 61761 (USA)

(Received 2 November 1992)

Abstract

The decomposition of $K_2[Co(C_2O_4)_2]$ occurs in two steps. The first occurs in the range 140–250°C and involves the loss of 1.5 moles of CO to produce $K_2[Co(C_2O_4)_{0.5}(CO_3)_{1.5}]$. Avrami rate laws with indices of 1.5 and 2 provide about equally good fits to most of the data. A gradual loss of CO continues up to about 350°C where the composition is $K_2[Co(CO_3)_2]$: this decomposes in a single step to K_2O and CoO by 430°C. This reaction gave α, T data, most of which were best represented by a power law, P3.

INTRODUCTION

The number of thermal studies that have been carried out on oxalates is very large. Both simple oxalates, e.g. MnC_2O_4 , $Ag_2C_2O_4$, and NiC_2O_4 , and oxalate complexes, e.g. $K_3[Co(C_2O_4)_3]$, $K_3[Mn(C_2O_4)_3]$, and $K_2[Ni(C_2O_4)_2]$, have received considerable attention. Space does not permit a complete review of this large body of literature. Many of the early studies on simple oxalates have been reviewed by Young [1]. Early studies on oxalate complexes include those of Wendlandt and Simmons on $K_3[Cr(C_2O_4)_3] \cdot 3H_2O$, $K_3[Co(C_2O_4)_3] \cdot 3H_2O$, and $K_3[Mn(C_2O_4)_3] \cdot 3H_2O$ [2–4]. Oxalate complexes of Ni(II), Co(II), and Cu(II) have also been studied [5]. Our early work on oxalates and oxalate complexes included studies on $K_3[Al(C_2O_4)_3]$ [6], $K_3[Fe(C_2O_4)_3] \cdot 2H_2O$ [7], $K_3[Cr(C_2O_4)_3] \cdot 3H_2O$ [7], $[Co(NH_3)_6]_2(C_2O_4)_3 \cdot 4H_2O$ [8], $Y_2(C_2O_4)_3 \cdot 9H_2O$, $Nd_2(C_2O_4)_3 \cdot 10H_2O$, $Ho_2(C_2O_4)_3 \cdot 5.5H_2O$ [9], $K_2[Co(C_2O_4)_2]$ [10], $K_3[Co(C_2O_4)_3]$ [10], and *cis*- and *trans*- $K[Cr(C_2O_4)_2(H_2O)_2]$ [11].

There have also been many more recent studies by a large number of workers [12]. In spite of the large body of literature that exists on the decomposition of both simple oxalates and oxalate complexes, there is much to be learned about these systems. Many of the studies were conducted before sophisticated instruments and comprehensive data-analysis techniques became available. We have shown that studies using

* Corresponding author.

such methodologies can be unreliable [13,14]. Consequently, we have chosen to reinvestigate the decomposition of $K_2[Co(C_2O_4)_2]$ using highly replicated studies and comprehensive data-analysis procedures in an effort to interpret more clearly the reactions involved. This report presents the results of that work.

EXPERIMENTAL

A sample of $K_2[Co(C_2O_4)_2]$ obtained from the Apache Chemical Company was used in this work without further treatment. Non-isothermal TG studies were carried out using a Perkin-Elmer TGS-7 which was controlled by a TAC-7 controller linked to an IBM PS/2 50Z computer. Samples were heated in a nitrogen atmosphere flowing at $50\text{ cm}^3\text{ min}^{-1}$, with heating rates of 2.5, 5.0, and $10.0^\circ\text{C min}^{-1}$. Four runs were made at each rate. The fraction of reaction completed, α , was determined as a function of temperature and the α , T data were analyzed by the method of Reich and Stivala [15]. The rate laws tested in this procedure are shown in Table 1.

TABLE 1

Rate laws tested

A4	$[-\ln(1-\alpha)]^{1/4}$	A3	$[-\ln(1-\alpha)]^{1/3}$
P3	$\alpha^{1/2}$	A2	$[-\ln(1-\alpha)]^{1/2}$
A1.5	$[-\ln(1-\alpha)]^{2/3}$	R2	$1-(1-\alpha)^{1/2}$
R3	$1-(1-\alpha)^{1/3}$	F1	$-\ln(1-\alpha)$
D1	α^2	D2	$\alpha+(1-\alpha)\ln(1-\alpha)$
D4	$1-(2\alpha/3)-(1-\alpha)^{2/3}$	D3	$[1-(1-\alpha)^{1/3}]^2$

RESULTS AND DISCUSSION

The decomposition of $K_2[Co(C_2O_4)_2]$ produced the typical TG curve shown in Fig. 1. In all the runs carried out, the TG curves obtained were virtually identical. Decomposition appears to be highly reproducible. The reaction



is accompanied by a mass loss that becomes very gradual after about 250°C , by which point the stoichiometry shown above is reached. This agrees reasonably well with the 13.5% mass loss observed for the first step in the

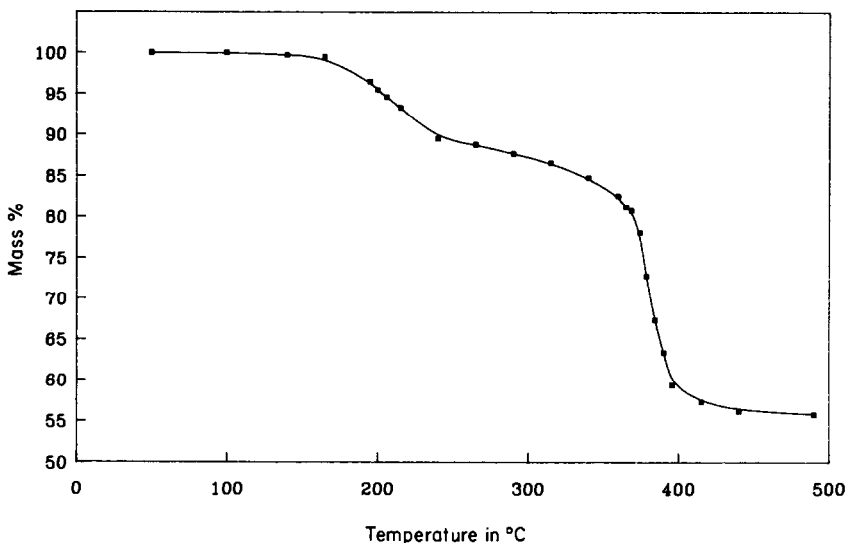
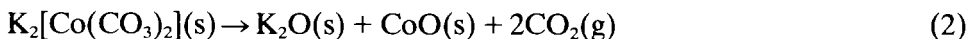


Fig. 1. TG curve for the decomposition of $K_2[Co(C_2O_4)_2]$.

TG curve in the range 140–250°C. Following this reaction, a gradual loss of CO continues until the mass appears to be that of $K_2[Co(CO_3)_2]$ at 360°C where the calculated and observed mass losses are 18%. This material decomposes according to the equation



in the temperature range 360–450°C. A mass loss of 28.2% is observed, while the value calculated according to eqn. (2) is 28.3%. The α , T data for the reactions shown in eqns. (1) and (2) were analyzed by the procedure of Reich and Stivala [15]. This method requires data from runs carried out at heating rates which differ by a factor of two. Therefore, heating rates of 2.5, 5.0, and 10.0°C min⁻¹ were selected. Because four runs were made at 2.5°C min⁻¹ and four at 5.0°C min⁻¹, 16 combinations of the data sets can be made. Also, four runs were made at 10°C min⁻¹, so that 16 combinations of data sets from the 5.0 and 10°C min⁻¹ runs were made. Using permutations of the data sets in this way provides the best assurance that results from one or two isolated runs do not obscure the general pattern of behavior. The results of analyzing these data for the reaction shown in eqn. (1) by the Reich and Stivala procedure [15] are shown in Table 2.

The reaction shown in eqn. (1) appears to follow an Avrami rate law with the A1.5 and A2 cases providing almost equally good fits to the data. The only other rate laws giving a better fit for a few specific combinations of data were P3, R3, and R2. These three rate laws accounted for 11 of the 32 run combinations, but the A2 and A1.5 rate laws gave the best fit in 21 of

TABLE 2

Kinetic analysis of data for the reaction shown in eqn. (1)

Run combination ^a	Best fit		Second-best fit	
	Rate law	S.E.E. ^b	Rate law	S.E.E.
Runs at 5.0 and 10.0°C min ⁻¹				
1A	P3	0.0232	A2	0.0325
1B	P3	0.0322	A2	0.0406
1C	P3	0.0334	A2	0.0431
1D	A2	0.0752	P3	0.0853
2A	A2	0.0115	P3	0.0222
2B	A2	0.0121	P3	0.0270
2C	A2	0.0101	P3	0.0238
2D	A2	0.0110	P3	0.0257
3A	A2	0.0157	P3	0.0193
3B	A2	0.0112	P3	0.0222
3C	A2	0.0123	P3	0.0196
3D	A2	0.0106	P3	0.0206
4A	A2	0.0609	P3	0.0705
4B	P3	0.0278	A2	0.0396
4C	A2	0.0593	P3	0.0699
4D	P3	0.0256	A2	0.0380
Runs at 2.5 and 5.0°C min ⁻¹				
AI	A1.5	0.0115	R2	0.1244
AII	A1.5	0.0466	R2	0.0483
AIII	R3	0.0201	R2	0.0221
AIV	A1.5	0.0562	A2	0.0765
BI	R2	0.0344	R3	0.0369
BII	A1.5	0.0403	R2	0.0632
BIII	R3	0.0241	R2	0.0244
BIV	A1.5	0.0591	A2	0.0891
CI	R2	0.0328	R3	0.0351
CII	A1.5	0.0094	R2	0.0831
CIII	R3	0.0209	R2	0.0214
CIV	A1.5	0.0575	A2	0.0862
DI	R2	0.0331	R3	0.0355
DII	A1.5	0.0599	A2	0.0681
DIII	A1.5	0.0577	A2	0.0751
DIV	A1.5	0.0546	A2	0.1012

^a Runs 1–4 were at 10°C min⁻¹; runs A–D were at 5.0°C min⁻¹; runs I–IV were at 2.5°C min⁻¹. ^b S.E.E. is the standard error of estimate.

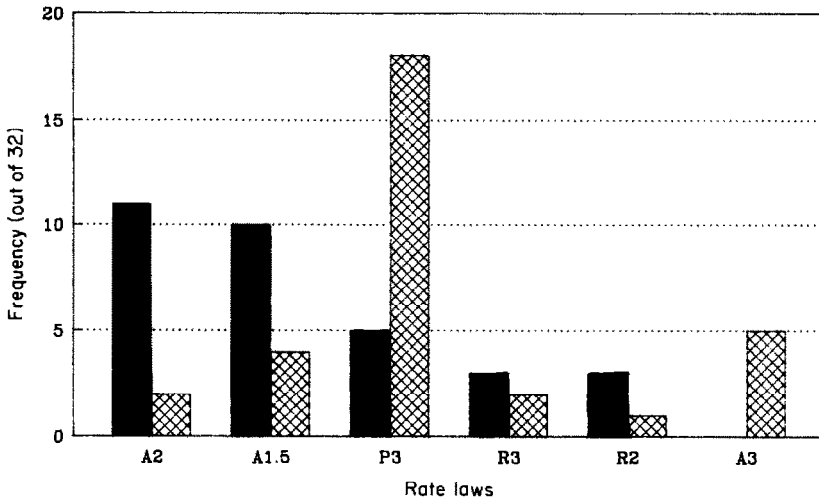


Fig. 2. Distribution diagram showing the best-fitting rate laws for reactions shown in eqn. (1) (solid bar) and eqn. (2) (crosshatched bar).

the 32 cases. It is readily apparent that kinetic studies on this process using the Coats and Redfern [16] procedure based on the rate law

$$\frac{d\alpha}{dt} = \frac{A}{\beta} (1 - \alpha)^n e^{-E/RT} \quad (3)$$

where the symbols have their usual meanings, cannot yield useful information because this rate law does not permit the Avrami rate law forms to be tested.

In order to demonstrate the range of rate laws indicated by the kinetic analysis and their frequency of occurrence, it is instructive to display such information graphically. Figure 2 shows the distribution of best-fitting rate laws as a bar graph for the reaction shown in eqn. (1) (solid bar). The dominance of the A1.5 and A2 rate laws in fitting the data is clearly shown.

Data for the reaction shown in eqn. (2) are presented in Table 3. For 18 of the 32 combinations, the power law P3 gave the best fit to the data. Eleven combinations indicated one of the Avrami rate laws (A3, five cases; A1.5, four cases; and A2, two cases) as providing the best fit to the data. It seems, however, that this reaction is best interpreted in terms of the P3 rate law. Figure 2 shows the dominance of this rate law for providing the best fit to the data for the reaction shown in eqn. (2).

The results of this work show that sample-to-sample variations, even in runs with almost identical TG curves, preclude determining a rate law by kinetic analysis of a small number of runs. Even when state-of-the-art equipment is used, data of accuracy and precision sufficient to choose between several mathematically similar rate laws are not necessarily

TABLE 3

Kinetic analysis of data for the reaction shown in eqn. (2)

Run combination ^a	Best fit		Second-best fit	
	Rate law	S.E.E. ^b	Rate law	S.E.E.
Runs at 5.0 and 10°C min ⁻¹				
5E	A3	0.0820	P3	0.1475
5F	A3	0.0667	P3	0.1587
5G	A3	0.0786	P3	0.1523
5H	A1.5	0.0610	R2	0.1059
6E	P3	0.0689	A2	0.0793
6F	P3	0.0751	A2	0.0793
6G	P3	0.0737	A2	0.0835
6H	A1.5	0.0606	R2	0.0778
7E	P3	0.0845	A2	0.0955
7F	P3	0.0950	A2	0.1079
7G	P3	0.0895	A2	0.1002
7H	P3	0.0919	A2	0.1051
8E	P3	0.0998	A3	0.1119
8F	A3	0.1014	P3	0.1162
8G	R2	0.0709	R3	0.0720
8H	P3	0.1022	A3	0.1108
Runs at 2.5 and 5.0°C min ⁻¹				
EV	A3	0.0954	P3	0.1058
EVI	R3	0.0615	F1	0.0678
EVII	A2	0.0470	P3	0.0583
EVIII	P3	0.0662	A2	0.0797
FV	P3	0.0543	A2	0.0643
FVI	P3	0.0539	A2	0.0667
FVIII	P3	0.0783	A2	0.0913
GV	P3	0.0859	A2	0.0984
GVI	P3	0.0269	A2	0.0414
GVII	A2	0.0432	P3	0.0593
GVIII	P3	0.0430	A2	0.0565
HV	P3	0.0783	A2	0.0909
HVI	P3	0.0272	A2	0.0407
HVII	A1.5	0.0399	R2	0.0729
HVIII	A1.5	0.0550	R2	0.0894

^a Runs 5–8 were at 10°C min⁻¹; runs E–H were at 5.0°C min⁻¹; runs V–VIII were at 2.5°C min⁻¹. ^b Standard error of estimate.

obtained. At the present time, it appears that the only way to achieve a consistent view of the rate law for a solid state process using TG data is to perform numerous experiments and to carry out kinetic analysis on permutations of the data sets. Even then, a sizeable number of cases will probably not obey the most frequently indicated rate law.

REFERENCES

- 1 D.A. Young, *Decomposition of Solids*, Pergamon Press, Oxford, 1966.
- 2 W.W. Wendlandt and E.L. Simmons, *Thermochim. Acta*, 2 (1971) 217.
- 3 E.L. Simmons and W.W. Wendlandt, *J. Inorg. Nucl. Chem.*, 27 (1965) 2325.
- 4 W.W. Wendlandt and E.L. Simmons, *J. Inorg. Nucl. Chem.*, 27 (1965) 2317.
- 5 D. Broadbent, D. Dollimore, and J. Dollimore, in R.F. Schwender, Jr. and P.D. Garn (Eds.), *Thermal Analysis*, Vol. 2, Academic Press, New York, 1969, pp. 739–760.
- 6 K.A. Foster and J.E. House, Jr., *Thermochim. Acta*, 60 (1983) 389.
- 7 J.E. House, Jr. and T.G. Blumthal, *Thermochim. Acta*, 36 (1980) 79.
- 8 G.L. Jeyaraj and J.E. House, Jr., *Thermochim. Acta*, 68 (1983) 201.
- 9 G.L. Jeyaraj and J.E. House, Jr., *Thermochim. Acta*, 71 (1983) 345.
- 10 J.E. House, Jr. and T.G. Blumthal, *Thermochim. Acta*, 43 (1981) 237.
- 11 J.E. House, Jr. and A.M. Learnard, *Thermochim. Acta*, 18 (1977) 295.
- 12 D. Dollimore and T.A. Evans, *Thermochim. Acta*, 179 (1991) 49.
- 13 J.E. House, Jr., *Thermochim. Acta*, 37 (1981) 379.
- 14 J.E. House, Jr. and L.A. Marquardt, *J. Solid State Chem.*, 89 (1990) 155.
- 15 L. Reich and S.S. Stivala, *Thermochim. Acta*, 62 (1983) 129.
- 16 A.W. Coates and J.P. Redfern, *Nature*, 201 (1964) 68.